HHS Public Access

Author manuscript

Oncogene. Author manuscript; available in PMC 2015 April 09.

Published in final edited form as:

Oncogene. 2014 October 9; 33(41): 4924–4931. doi:10.1038/onc.2013.431.

A reciprocal role of prostate cancer on stromal DNA damage

Jheelam Banerjee[3,*], **Rajeev Mishra**[1,*], **Xiaohong Li**[3], **Roger S. Jackson 2nd**[3], **Adrija Sharma**[4], and **Neil A. Bhowmick**[1,2]

[1]Department of Medicine, Cedars-Sinai Medical Center, Los Angeles, CA, USA

[2]Greater Los Angeles Veterans Administration, Los Angeles, CA, USA

[3]Department of Urology, Vanderbilt University, Nashville TN, USA

[4]Department of Mechanical, Aerospace and Biomedical Engineering, University of Tennessee, Knoxville, TN, USA

Abstract

DNA damage found in prostate cancer-associated fibroblasts (CAF) promotes tumor progression. In the absence of somatic mutations in CAF, epigenetic changes dictate how stromal co-evolution is mediated in tumors. Seventy percent of prostate cancer patients lose expression of transforming growth factor-beta type II receptor (*TGFBR2*) in the stromal compartment (n = 77, p value = 0.0001), similar to the rate of glutathione S-transferase P1 (GSTP1) silencing. Xenografting of human prostate cancer epithelia, LNCaP, resulted in the epigenetic *Tgfbr2* silencing of host mouse prostatic fibroblasts. Stromal *Tgfbr2* promoter hypermethylation initiated by LNCaP cells was found to be dependent on IL-6 expression, based on neutralizing antibody studies. We further found that pharmacologic and transgenic knockout of TGF-β responsiveness in prostatic fibroblasts induced *Gstp1* promoter methylation. It is known that TGF-β promotes DNA stability, however the mechanism is not well understood. Both prostatic human CAF and mouse transgenic knockout of Tgbr2 had elevated DNA methyltransferase I (DNMT1) activity and histone H3 lysine 9 trimethylation (H3K9me3) to suggest greater promoter methylation. Interestingly, the conditional knockout of *Tgfbr2* in mouse prostatic fibroblasts, in modeling epigenetic silencing of *Tgfbr2*, had greater epigenetic gene silencing of multiple DNA damage repair and oxidative stress response genes, based on promoter methylation array analysis. Homologous gene silencing was validated by RT-PCR in mouse and human prostatic CAF. Not surprisingly, DNA damage repair gene silencing in the prostatic stromal cells corresponded with the presence of DNA damage. Restoring the expression of the epigenetically silenced genes in wild type fibroblasts with radiation-induced DNA damage reduced tumor progression. Tumor progression was inhibited

Corresponding author: Dr. Neil A. Bhowmick, Samuel Oschin Comprehensive Cancer Institute, Cedars-Sinai Medical Center, 8750 Beverly Blvd., Atrium 103, Los Angeles, CA 90048, bhowmickn@cshs.org, Tel: (310) 871-4697.

*authors of equal contribution

The current addresses of the following authors are the following:

JB: Department of Biomedical and Diagnostic Sciences, University of Tennessee, Knoxville, TN, USA

XL: Van Andel Institute, Grand Rapids, MI, USA

Conflict of interest

The authors declare no conflicts of interest.

even when epigenetic silencing was reversed in the *Tgfbr2* knockout prostatic fibroblasts. Thus, fibroblastic epigenetic changes causative of DNA damage, initiated by association with cancer epithelia, is a dominant mediator of tumor progression over TGF-β responsiveness.

Keywords

stromal co-evolution; prostate cancer; TGF-beta; IL-6; DNA methylation

Introduction

Prostate cancer is the most commonly diagnosed cancer, next to skin cancer, in men and is increasing in incidence with the expanding aging population. As premalignant lesions progress to primary adenocarcinomas, then to metastatic and hormone refractory disease, somatic genomic lesions continue to accumulate within the cancer cells. Dynamic interaction between cancer cells and the host stromal fibroblastic microenvironment supports epithelial transformation, growth, and dissemination (1–3). The importance of the stroma is highlighted in histological observations of prostate cancer (PCa), with an expansion of myofibroblasts or activated stroma, primarily as a result of resident smooth muscle differentiation (4). The urogenital mesenchyme is inductive for prostatic gland development, as are cancer-associated fibroblasts (CAF) for epithelial tumor initiation (5, 6). Interestingly, experimental systems demonstrating the enhanced tumorigenic properties of CAF, attributed to androgen and transforming growth factor-beta (TGF-β) dependent paracrine factors, were all performed following the expansion of the cells *ex vivo* prior to grafting with epithelia (1, 5, 7). Thus, we hypothesized that in the absence of clonal mutations in CAF populations (8, 9), DNA methylation could mediate prostate tumor progression in a TGF-β dependent manner. This would support observed epigenetic change in prostatic fibroblast in the form of promoter methylation (10).

DNA damage in CAF is associated with greater cancer aggressiveness, attributed to DNA damage-associated secretory (DDS) phenotype (11, 12). Oxidative stress, toxic byproducts, reduced mitochondrial function, and external exposures to chemotherapy/radiation all brings about damage DNA in the stroma. Inefficient repair of DNA lesions can promote epithelial cell transformation and tumorigenesis, however stromal fibroblasts seem to die or under go a senesence phenotype in a context dependent manner (12, 13). The DDS phenotype, found in part in CAF overlap with the senecent fibroblasts secretome (12, 14). Importantly, the CAF exhibiting the DDS phenotype are not necessarily senecent. The tumor inductive phenotype of CAF cells can be maintained in culture temporarily (5). Thus, the cancer epithelial can impart the tumor inductive capacity of CAF. Interestingly, we find that cancer epithelia-derived paracrine factor mediates the loss of TGF-β signaling in the adjacent fibroblasts by silencing the TGF-β receptor type II (Tgfbr2) expression.

Mechanisms of DNA damage repair include the activation of the TGF-β pathway (15). TGF-β signal through downstream receptor-activated Smad-dependent and -independent pathways and, thereby, impacts many cell functions, including proliferation, apoptosis, and extracellular matrix deposition (16). Somatic inactivating mutations of Tgfbr2 are

demonstrated in several different tumor epithelia (17). However, PCa epithelia do not lose Tgfbr2 expression as often as associated fibroblastic cells (18). We found that the observed down regulation of Tgfbr2 in prostatic CAF to be an epigenetic phenomena. We developed transgenic mouse models with a conditional knockout of Tgfbr2 in a subset of stromal fibroblasts ($Tgfbr2^{fspKO}$ and $Tgfbr2^{ColTKO}$), which spontaneously result in PCa, express a DDS phenotype (1, 14, 19). Here we demonstrate that disruption of Tgfbr2 gene expression in fibroblastic cells support cancer progression through silencing of reactive oxygen metabolizing and DNA damage repair genes, suggesting a sequence of stromal evolution in its association with cancer epithelia. Evidence of epigenetic silencing of GSTP-1 and MyoD1 in the stromal compartment in the form of promoter methylation in human stromal cells is associated with PCa (10). It seems that the loss of Tgfbr2 expression may be a precursor to these common stromal promoter methylation events. Because of their reversible nature, epigenetic alterations are targeted therapeutically. Limiting stromal DNA methylation was found to prevent tumor progression, often attributed to stromal DNA damage. In coming full circle, we examined a candidate epithelia-derived mediator that lead to the observations of stromal TGF-β signaling down regulation and ensuing DNA damage.

Results

Based on previous identification of Tgfbr2 down regulation in CAF of PCa tissues and evidence of stromal epigenetic alterations (10, 18), we investigated the potential for *TGFBR2* promoter methylation in PCa progression. We utilized *GSTP1* promoter methylation as a positive control, for its reported methylation status in both epithelial and stromal compartments in 90% of PCa subjects (10). We independently isolated the epithelia and associated stromal compartments from PCa (N=33) and BPH (N=10) paraffin tissues by laser capture micro-dissection. The promoter methylation of *GSTP1* and *TGFBR2* was not detectable in benign prostate hyperplasia (BPH) patient tissues in either the epithelia or the stroma (Figure 1A). Both the epithelial and stromal compartments of the PCa tissue had evidence of *GSTP1* promoter methylation (data not shown, (10)). However, *TGFBR2* promoter methylation was more prevalent in the stroma than the epithelia in the PCa tissues. The level of association between PCa associated CAF and BPH samples computed using Chi-square and student's T-test values was determined to be highly significant.

The findings described for human PCa were replicated in the mouse models for PCa with conditional fibroblastic knockout of *Tgfbr2*. *Gstp1* promoter methylation was found in $Tgfbr2^{fspKO}$ prostatic stromal cells, but not observed in control prostatic stromal cells of $Tgfbr2^{floxE2/floxE2}$ mice (Figure 1B). Prostatic fibroblasts cultured from transgenic mice with a tamoxifen inducible Cre-driven by the Collagen Ia2 promoter, $Tgfbr2^{ColTKO}$ mice (19), similarly had methylated *Gstp1* 72 hours following 4-OH tamoxifen treatment. This was reaffirmed when $Tgfbr2^{floxE2/floxE2}$ cells were treated with TGF-β antagonist, LY364947 for 48 hours, and methylation of *Gstp1* was observed. Band intensity was measured for the methylation specific PCR experiments and statistical analysis was performed. Highly significant (p value < 0.001) differences were observed between the control and treated groups. The direct correlation of TGF-β signaling and *Gstp1* methylation studies in mouse prostatic fibroblasts suggested that the coincident observation of *TGFBR2* and *GSTP1* promoter methylation in men with PCa was a result of TGF-β regulation of the

GSTP1 methylation event. Accordingly, it was not surprising to find promoter methylation of both *Gstp1* and *Tgfbr2* in wild type mouse prostatic stromal cells associated with orthotopically xenografted human PCa epithelia, LNCaP (Figure 1B). Host fibroblast promoter methylation was determined through the use of mouse-specific methylation-specific PCR primers. As previous reports suggest the capacity of IL-6 to promote nuclear localization of DNMT1 and PCa (including LNCaP) are known to express elevated IL-6 (20, 21), we chose to test this mechanism in prostatic stromal cells exposed to LNCaP conditioned media. We found that LNCaP conditioned media with control IgG resulted in nuclear localization of Dnmt1 in wild type prostatic fibroblasts, as expected. However, the addition of IL-6 neutralizing antibody to LNCaP conditioned media did not significantly reduce nuclear Dnmt1 expression compared to IgG (Figure 1C). Interestingly, cytoplasmic Dnmt1 expression was elevated upon IL-6 neutralization, to result in a reduced ratio of nuclear Dnmt1 following IL-6 neutralization. More importantly, we found that IL-6 neutralization prevented Tgfbr2 promoter hypermethylation by LNCaP conditioned media (Figure 1D). The observed epithelial regulation of stromal epigenetic status supported further mechanistic interrogation.

The DNA methylation status of CAF seemed to be TGF-β dependent. DNA methyltransferase (DNMT) activity was measured in mouse prostatic fibroblasts with intact TGF-β signaling and those with Tgfbr2 knocked out, in parallel with human NAF and CAF cultured cells. We found 4-fold greater DNMT1 activity in prostatic fibroblasts knocked out for *Tgfbr2* (Tgfbr2-KO) compared to Tgfbr2-flox stroma (Figure 2A). Human CAFs similarly had over 4-fold greater Dnmt1 activity compared to normal tissue-associated fibroblasts (NAFs). However, there was little observed difference in DNMT3b activity in the respective mouse and human counterparts. Interestingly, protein expression of Dnmt1 was three-fold greater in Tgfbr2-KO over Tgfbr2-flox cells, in the absence of DNMT1 mRNA expression differences (Figure 2B). The elevation of DNMT1 protein expression in part presumably accounted for the increased DNMT1 activity observed in Tgfbr2-KO prostatic stromal cells.

Dnmt1 expression is reported to peak during the S and G2 phases of the cell cycle and is prone to proteasome-mediated degradation (22). We found DNMT1 was degraded by the proteosomal pathway on treatment with the protein synthesis inhibitor, cycloheximide (Chx), in Tgfbr2-flox fibroblasts, as compared to Tgfbr2-KO fibroblasts (Figure 2C). Densitometric quantitation of the Western blots indicated a significantly higher Tgfbr2-KO fibroblastic Dnmt1 protein expression compared to that of Tgfbr2-flox cells in the presence or absence of Chx (p value < 0.001). The inhibition of proteasome activity by MG132 with Chx treatment resulted in the recovery of DNMT1 expression. TGF-β regulation of DNMT1 protein stability and DNA methylation in the prostatic fibroblasts was part of the mechanism for elevated *Gstp1* promoter hypermethylation. Results suggested DNMT1 to be down regulated by TGF-β in a post-translational manner.

CpG hypermethylation and repressive chromatin modifications are associated with methylated histone H3 that has been trimethylated on either lysine 9 (H3K9me3) or lysine 27 (H3K27me3) and H3K9 de-acetylation. Immunofluorescence nuclear localization of H3K9me3 was prominent in prostatic mouse Tgfbr2-KO and human CAF cells, compared to

their respective Tgfbr2-flox and NAF counterparts (Figure 3A). Western blotting demonstrated elevated H3K9me3 and reduced histone H3 lysine 9 acetylation (H3K9Ac) in both $Tgfbr2^{fspKO}$ and $Tgfbr2^{ColTKO}$ prostatic fibroblasts compared to control $Tgfbr2^{floxE2/floxE2}$ fibroblasts (Figure 3B). Parallel to that seen with mouse fibroblasts, the expression pattern of H3K9me3 was elevated in CAFs with a reduced expression of H3K9Ac, relative to the control NAFs (Figure 3C). Densitometry of the blots indicated highly significant differences in the expression of H3K9me3 and H3K9Ac between the NAF's and the CAF's (p value < 0.001). Further chromatin immunoprecipitation (ChIP) analysis suggested, that the elevated Dnmt1 activity in Tgfbr2-KO fibroblasts was associated with 8-fold greater *Gstp1* promoter loading compared to Tgfbr2-flox cells (Figure 3D). Analogously, significantly elevated H3K9me3 and reduced H3K9Ac bound the *Gstp1* promoter in Tgfbr2-KO cells, compared to Tgfbr2-flox cells, supporting the observed *GSTP1* methylation in PCa-associated stromal fibroblasts.

With the goal of determining the role of TGF-β-mediated epigenetic regulation, methylation array analysis was performed on Tgfbr2-flox and Tgfbr2-KO fibroblastic cells from six independent mouse prostates. The results of the gene cluster analyses showed that Tgfbr2-KO fibroblasts had greater number of genes methylated with elevated methylation per gene (peak scores), compared to Tgfbr2-flox (Figure 4). Each data point in the plot represents the average peak score of methylated peaks, with approximately eight promoter regions for each gene analyzed. In a distribution of gene clusters plotted against average peak scores, those clusters of genes with the greatest number of methylated sites were segregated. The data distinctly revealed DNA damage repair and reactive oxygen species metabolizing gene promoter hypermethylation in Tgfbr2-KO compared to Tgfbr2-flox fibroblasts. Eleven of sixteen genes were functionally verified to be silenced in Tgfbr2-KO fibroblastic cells compared to Tgfbr2-flox through qRT-PCR (Figure 5A). The silenced genes were found to be re-expressed following treatment with methyltransferase inhibitors 5-aza-2′-deoxycytidine (5-aza-dC). Fifteen human homologs of the selected mouse genes, were epigenetically silenced in prostatic CAF cultured from primary tumors compared to their paired NAF from ten independent PCa patients (Figure 5B). The difference between Tgfbr2-KO and Tgfbr2-KO+5-AZA groups was found to be highly significant (p value < 0.001), as were the difference between CAF and CAF+5AZA (p value < 0.0001). DNA double stranded breaks (DSB) are normally corrected through base excision repair, nucleotide excision repair, and homologous recombination. We had further evidence that the epigenetic silencing by the loss of TGF-β responsiveness was DNMT-dependent, based on the treatment of Tgfbr2-KO fibroblasts with the DNMT-selective inhibitor, RG108. Methylation-sensitive restriction enzyme digestion and PCR for two homologous recombination candidate promoters for Xrcc2 and Rad50 were not found to be methylated following RG108 treatments (Supplemental Figure 1). Genes in each category of DSB repair were silenced in Tgfbr2-KO and CAF cells. Upon broader analysis we also found there were several human PARP genes methylated including PARP3, PARP8, PARP9 and PARP12, however, PARP16 was chosen to represent this family of DSB repair genes. Protein detection of PARP1 (involved in base excision repair) and Ku70 (associated with NHEJ, non-homologous end-joining repair) in prostatic fibroblasts following TGF-β antagonism further supported the involvement of base excision repair (Figure 5C). We treated human

NAF with the TGF-β antagonist, LY36497, for a time course of 0, 12, 24, 48 and 72 hours. Previous gene expression analysis indicated DSB repair genes to be a prominent subset down regulated in PCa reactive stroma, compared to benign epithelia associated stroma from the same patients (23). The expression of PARP1 was down regulated by LY36497, whereas no significant decrease in Ku70 expression was detected even after following prolonged treatment. Thus, base excision repair and homologous recombination are consequential pathways suppressed in prostatic CAF in a TGF-β dependent mechanism.

The consequence of stromal epigenetic changes on epithelial tumor progression was next tested. The biologic consequence of down regulating the DNA repair mechanisms was hypothesized to be an accumulation of stromal DNA damage. In fact, we found that epigenetic silencing of DNA damage repair genes as a result of knocking out Tgfbr2 resulted in stromal γ-H2AX and Rad52 expression, comparable to that found in wild type fibroblasts subjected to 8 Gy irradiation (Supplemental Figure 2A). In parallel, primary cultures of CAF demonstrated elevated stromal DSB, compared to NAF, γ-H2AX foci localization (Supplemental Figure 2B). PCa tissues also had greater DSB compared to benign prostatic stroma. Thus, the loss of TGF-β responsiveness in prostatic stroma can result in accumulation of DNA damage. Irradiated (8Gy) wild type mouse prostatic stromal cells (as a cancer-independent means of DSB induction) were recombined with castrate-resistant PCa, C42b epithelia. Compared to C42b alone or recombinants with non-irradiated prostatic stroma, not surprisingly the irradiated stromal cell containing recombinants developed the largest tumors (n = 28, Table 1, Supplemental Figure 3). However, tissue recombinants generated with irradiated wild type prostatic stromal cells subjected to 5-aza-dC treatment developed significantly smaller tumors. Phosphorylated histone H3 staining of mitotic cells correlated with the orthotopic tumor volumes measured. The results supported the prevalence of stromal DNA damage and loss of *Tgfbr2* expression in PCa progression. However, the treatment of Tgfbr2-KO fibroblastic cells with 5-aza-dC prior to recombination with LNCaP cells resulted in significantly smaller tumors, to control LNCaP cells alone and Tgfbr2-KO fibroblasts not treated with 5-aza-dC (n = 18, Table 1, Supplemental Figure 4). The loss of fibroblastic Tgfbr2 expression did not potentiate tumor progression when DNA methylation resulting from it was reversed with 5-aza-dC treatment. This suggested DSB in inductive CAF (12, 24), can be epigenetically regulated in a TGF-β-dependent manner. Together, PCa epithelia can mediate epigenetic changes in adjacent stromal cells resulting in accumulation of DNA damage in a TGF-β dependent manner, to in turn potentiate the CAF phenotype for further tumor progression.

Discussion

Somatic genomic lesions, including mutations, translocations, amplifications, and deletions, are characteristic of cancer epithelia (11, 25, 26). However, no such clonal genomic changes were observed in prostatic CAF (8, 9). The dynamic interaction between the neoplastic epithelia and adjacent stromal fibroblastic cells contributing to a co-evolution of the two compartments is well recognized (23, 27), as are alterations in epigenetic regulation associated with initiating events in cancer development (10, 28). Here we demonstrate a common cancer epithelia-derived cytokine, IL-6, can contribute to the epigenetic silencing of Tgfbr2 in adjacent fibroblastic cells (Figure 5D). Such a loss of prostatic stromal TGF-β

signaling can mediate the further epigenetic silencing of DNA damage repair and reactive oxygen metabolizing enzymes (Figures 4 and 5). The loss of stromal TGF-β signaling is associated with spontaneous prostatic tumor initiation, epigenetic down regulation of DNA damage repair genes, and exhibit features of a DDS phenotype (1, 12, 14). Such changes can be considered a component of the co-evolving events that occur in the fibroblasts as part of a reciprocal communication between the tumor and stromal compartments.

Intriguingly, the epigenetic loss of *TGFBR2* expression in prostatic fibroblasts, initiated by interactions with PCa (Figure 1), results in the promoter methylation and silencing of DNA damage repair mediators (12, 18, 24). We found that *GSTP1*, a prototypical methylated gene in cancer epithelia and CAF, can be initiated by the loss of TGF-β responsiveness. We found that *TGFBR2* silencing in prostatic CAF, while present in majority of PCa subjects (18), was not essential if stromal DNA damage is initiated (Table 1B, Supplemental Figure 4). Based on previous studies, mouse prostatic fibroblasts knocked out for *Tgfbr2* exhibit a secretory phenotype similar to the DDS phenotype in irradiated, reactive oxygen species exposed, and senescent human prostatic fibroblasts (12, 14, 29). Here, we demonstrated that TGF-β responsiveness negatively regulates post-translational DNMT1 stability in prostatic fibroblasts, supporting the elevated DNMT1 activity identified in CAF (Figures 1 and 2). The mechanism of DNA damage repair and reactive oxygen metabolizing gene's epigenetic targeting by *TGFBR2* silencing is not known. However, Dumont et al. previously demonstrated DNA methylation as a semi-permanent means of gene silencing determined by more transitory transcriptional repressors (30). Thus, pathways associated with *TGFBR2* silencing could initiate transcriptional repressive cascades, potentially directing DNMT1 targeting of the identified genes. In human cancer epithelia, DNMT1 and DNMT3b cooperatively maintain DNA methylation and gene silencing, where disruption of either have minimal effects on cancer epigenetics. Interestingly, DNMT3b activity was not appreciably affected by silencing TGF-β signaling in either mouse of human prostatic fibroblasts (Figure 1). DNMT1 post-translational regulation by TGF-β in prostatic CAF is a determinant of DNA damage and ensuing paracrine mediator of cancer progression.

Accumulating data support the stromal DNA damage to be a significant mediator of adjacent tumor progression. Unlike genetic alterations, epigenetic changes are reversible. Therapeutics targeting global DNA methylation, such as 5aza-dC has been used in patients with myeloid leukemia and myelodysplastic syndrome (AML/MDS) for some time (31, 32). DNMT antagonists are similarly being tested in solid tumors (33). The methylation array analysis suggested that there is a significant global hypermethylation that occurs in CAF in TGF-β dependent manner (Figure 4). The use of tissue recombination techniques allowed us to demonstrate that hypomethylation of only the stromal fibroblastic cells can reduce the tumorigenesis of established castrate dependent and resistant PCa epithelia. A rational for selectively avoiding de-methylating genes on cancer epithelia would be to prevent activating oncogenes. *In vivo* stromal targeting of therapeutics could be envisioned through the use of antibodies directed towards unique cell surface proteins. As DNA and histone modifications are inter-dependent, HDAC inhibitors may be better suited for stromal targeting. Such therapeutic strategies would result in preventing stromal DNA damage and likely inhibit tumor progression.

The studies support the fact that TGF-β safeguards DNA fidelity by epigenetic regulation in fibroblastic cells. Microsatellite unstable colon cancer serves as a model for a mutation in the *TGFBR2* gene associated with the loss of DNA damage repair gene expression and epithelial genetic instability (34, 35). The DNA damage status of the irradiated stroma did not change due to 5-aza-dC treatment alone. However, 5-aza-dC treatment resulted in C42b-associated irradiated stroma to maintain Tgfbr2 expression and diminished DNA DSB at the time of tumor analysis after 8 weeks of grafting. The innate ability of DNA damage repair was restored by 5-aza-dC treatment (Table 1, Supplemental Figure 3, 4). The role of inflammatory immune response to DDS candidate factors, such as IL-1β, IL-6, and SDF1 are not accounted for in the tumor progression, as the tissue recombination studies were performed in immune-compromised mice. Here we find that stromal factors like IL-6 can also act on adjacent fibroblasts and in turn cancer epithelia. Future experiments testing the role of DDS on the host immune response are needed. The role for TGF-β responsiveness in prostatic CAF on cancer progression is interestingly complex, but is reproducibly one of tumor suppression.

Materials and Methods

Animals and Cultured Cells

$Tgfbr2^{floxE2/floxE2}$, $Tgfbr2^{ColTKO}$, and $Tgfbr2^{fspKO}$ mice were maintained as previously described (1, 19, 36). Primary mouse prostate stromal cell cultures were generated from 6–8-week-old $Tgfbr2^{floxE2/floxE2}$, $Tgfbr2^{ColTKO}$, and $Tgfbr2^{fspKO}$ mice as before (7). CAF and NAF cells were similarly developed from fresh human prostatectomy tissues. Mouse and human stromal primary cultures were used in the first seven passages. LNCaP and C42b cells (from ATCC) were recombined with prostatic stromal cells in the ratio of 100,000: 300,000 and grafted orthotopically into the anterior prostate of 4-week old male severe combined immunodeficient (SCID, Harlan, Indianapolis, IN, USA) (18). The tumors were harvested, photographed and processed for histologic evaluation. Institutional Animal Care and Use Committee and Institutional Review Board at Vanderbilt University and Cedars-Sinai Medical Center approved the procedures.

Antibodies, Immunohistochemistry, and Immunofluorescence

Paraffin-embedded tissue sections (5 mm) were deparaffinized and hydrated through xylene and graded alcohols using a standard protocol. Immunohistochemical staining used antibodies against phosphorylated-histone H3 (1:1000, Upstate, Temecula, CA), gamma-H2AX (1:250, Trevigen) and H3K9me3 (1:250, Abcam). Appropriate HRP-conjugated secondary antibodies and DAB incubation (Dako North America, Carpinteria, CA) or Cy3-conjugated secondary antibody (Invitrogen) were used for visualization. Western blots, separated by 10% SDS–polyacrylamide gels were incubated with primary antibodies for H3K9me3, H3K9Ac, or β-actin (Santa Cruz) overnight at 4°C, for subsequent standard ECL plus Western blotting detection (GE Healthcare).

IL-6 Antibody Neutralization

LNCaP CM was collected by aspiration, centrifuged to remove cell debris, prior to addition to prostatic fibroblasts in the presence or absence of IL-6 neutralizing antibody (MAB-206;

R&D system, 150 ng) or control IgG antibody. Fresh RPMI media served as control. After incubation for 48 hr cells were collected for nuclear and cytoplasmic fractionation (NE-PER Nuclear and Cytoplasmic Extraction Kit, Thermo Scientific) for Western blot expression analysis. Alternatively, DNA was extracted from prostatic stromal cells for methylation PCR analysis.

Quantitative Reverse Transcription–PCR, ChIP Analysis, and Methylation Specific PCR

RNA was extracted using the RNAeasy mini kit (Qiagen, Valencia, CA) according to the manufacturer's protocol. Relative quantitation relative to 18s rRNA expression was calculated by ΔΔCt method following reverse transcription and quantitative real-time PCR as before (37). ChIP analysis of the GSTP1 promoter in Tgfbr2-flox and Tgfbr2-KO prostate stromal cells were performed as described previously (37). Chromatin fragments were immunoprecipitated with DNMT1, H3K9me3, or H3K9Ac antibody and normal mouse IgG as negative control overnight at 4°C. Further steps followed the protocol from the EZ Chip kit (Upstate). Methylation specific PCR was performed with 50–100ng of DNA for bisulfite treatment (EZ DNA Methylation Direct Kit, Zymo Research). Subsequently, the modified DNA (2ul-4ul) was used as a template for PCR (38).

DNMT1 Activity Assay

The EpiQuik™ DNA Methyltransferase Activity/Inhibition Assay Kit (Epigentek) was used for measuring total DNMT activity (de novo, maintenance). The assay was performed according to the manufacturer's protocol and the data was normalized to the controls and computed.

DNMT inhibition in Tgfbr2-knockout fibroblasts

Cells were treated with established small molecule inhibitors of DNMT, RG108 (Sigma) or DMSO (vehicle control) for 5 days. Genomic DNA was isolated from (QIAGEN) genomic DNA (1 μg) from each group were digested using EpitTect methyl II DNA restriction Kit (QIAGEN) according to the manufacturer's instructions. Obtained DNA fragment (Mo: Control and Ms: un-methylated) methylation status at the promoter region of damage repair genes such as Rad50 and Xrcc2, DNA was assessed by methylation-specific PCR.

Methylation Array

Two methylated DNA enrichment methods were used prior to array hybridization. Genomic DNA from three biological replicates of each sample was prepared (Qiagen Dnaeasy Kit). Immunoprecipitated using a monoclonal antibody against 5-methylcytidine (MeDIP, Eurogentec) was performed on sonicated DNA as described previously for genome-wide promoter array analysis (39). Alternatively, sonicated DNA was subjected to Methyl Miner system of methyl-binding protein 2 (MBD2)-mediated pull down (Invitrogen). Following similar target labeling (6 μg) for both methylated DNA enrichment methods, DNA was hybridized to MM8_CpG_Island_Pro, OID17350 arrays (19,489 mouse promoters, Nimblegen) and scanned on Axon 4000B scanner following standard protocols. The rate of false positives was reduced by dual hybridization to the array subtracting input DNA with

both methods of methylated DNA enrichment and standard dye-swapping techniques. Data analysis was performed using Nimblescan 2.5 software.

Statistical Analysis

All test of significance were two-sided and were performed at a 95% confidence level using statistical software Jmp (SAS Institute Inc.). Level of significance for all tests was determined at $p \leq 0.05$. Chi-square values and student's T-test values were computed to determine the level of association between PCa and the methylation of Tgfbr2 and GSTP1 genes (Figure 1A). Band intensity of the samples for methylation specific PCR (Figure 1B) was measured using Image J (http://rsbweb.nih.gov/ij/). ANOVA and Tukey Kramer multiple comparison tests using GraphPad Instat software (GraphPad Software Inc., La Jolla, CA, USA) was performed to test differences between FloxE2, Tgfbr2KO and ColTKO groups and p value was computed. Statistical significance of differences between six densitometric readings per protein band from three independent Western blots for the semi-quantitative assessment of H3K9me3 and H3K9Ac Figure (3A and 3B) prepared from three randomly selected samples was assessed by the non-parametric Mann-Whitney test and p-value was computed using GraphPad Instat software. Similar statistical analysis was performed for Figure 3D. Cluster analysis was performed using Matlab (MathWorks Inc.) in order to identify the differences in peak score between the WT and the KO and also to compute differential peak scores amongst genes (Figure 4). K-means clustering was used to find clusters of comparable spatial extent, while the expectation-maximization mechanism allowed clusters to have different shapes. Variance was used as a measure of cluster scatter with Euclidian distance as a metric. Diagnostic checks were run on the datasets to avoid false results. Venny (40) was used for the Venn diagrams comparing groups (Figure 4). The tumor volume and mitotic index data for the orthotopic xenografts (Table 1A and 1B) was first tested for normality using the Shapiro-Wilk test. When the data was found to be normal, parametric test one-way ANOVA was used to compute the summary of fit. For pairwise comparisons among the groups parametric one-way analysis of variance was used and Tukey–Kramer multiple comparison test was used for pairwise comparison between groups. Tumor volumes and phosphorylated-histone H3 positive staining were averaged and standard deviations calculated (Supplemental Figures 3 & 4). RNA expression was calculated by ΔΔCt method (Figure 5) and Two-Way ANOVA was performed on the grouped data using GraphPad Prism (GraphPad Software Inc., La Jolla, CA, USA).

Supplementary Material

Refer to Web version on PubMed Central for supplementary material.

Acknowledgments

The work was supported by R01CA108646 (to NAB) from the National Cancer Institute.

References

1. Bhowmick NA, Chytil A, Plieth D, Gorska AE, Dumont N, Shappell S, et al. TGF-beta signaling in fibroblasts modulates the oncogenic potential of adjacent epithelia. Science. 2004; 303(5659):848–51. Epub 2004/02/07. [PubMed: 14764882]

2. Bhowmick NA, Neilson EG, Moses HL. Stromal fibroblasts in cancer initiation and progression. Nature. 2004; 432(7015):332–7. Epub 2004/11/19. [PubMed: 15549095]

3. Nguyen DX, Bos PD, Massague J. Metastasis: from dissemination to organ-specific colonization. Nat Rev Cancer. 2009; 9(4):274–84. Epub 2009/03/25. [PubMed: 19308067]

4. Tuxhorn JA, Ayala GE, Smith MJ, Smith VC, Dang TD, Rowley DR. Reactive stroma in human prostate cancer: induction of myofibroblast phenotype and extracellular matrix remodeling. Clin Cancer Res. 2002; 8(9):2912–23. [PubMed: 12231536]

5. Olumi AF, Grossfeld GD, Hayward SW, Carroll PR, Tlsty TD, Cunha GR. Carcinoma-associated fibroblasts direct tumor progression of initiated human prostatic epithelium. Cancer Res. 1999; 59(19):5002–11. [PubMed: 10519415]

6. Cunha GR. Androgenic effects upon prostatic epithelium are mediated via trophic influences from stroma. Prog Clin Biol Res. 1984; 145:81–102. [PubMed: 6371832]

7. Placencio VR, Sharif-Afshar AR, Li X, Huang H, Uwamariya C, Neilson EG, et al. Stromal transforming growth factor-beta signaling mediates prostatic response to androgen ablation by paracrine Wnt activity. Cancer Res. 2008; 68(12):4709–18. Epub 2008/06/19. [PubMed: 18559517]

8. Qiu W, Hu M, Sridhar A, Opeskin K, Fox S, Shipitsin M, et al. No evidence of clonal somatic genetic alterations in cancer-associated fibroblasts from human breast and ovarian carcinomas. Nat Genet. 2008; 40(5):650–5. [PubMed: 18408720]

9. Campbell I, Polyak K, Haviv I. Clonal mutations in the cancer-associated fibroblasts: the case against genetic coevolution. Cancer Res. 2009; 69(17):6765–8. discussion 9. Epub 2009/08/27. [PubMed: 19706773]

10. Jeronimo C, Usadel H, Henrique R, Oliveira J, Lopes C, Nelson WG, et al. Quantitation of GSTP1 methylation in non-neoplastic prostatic tissue and organ-confined prostate adenocarcinoma. J Natl Cancer Inst. 2001; 93(22):1747–52. Epub 2001/11/22. [PubMed: 11717336]

11. Lengauer C, Kinzler KW, Vogelstein B. Genetic instabilities in human cancers. Nature. 1998; 396(6712):643–9. [PubMed: 9872311]

12. Coppe JP, Patil CK, Rodier F, Sun Y, Munoz DP, Goldstein J, et al. Senescence-associated secretory phenotypes reveal cell-nonautonomous functions of oncogenic RAS and the p53 tumor suppressor. PLoS Biol. 2008; 6(12):2853–68. Epub 2008/12/05. [PubMed: 19053174]

13. Ohuchida K, Mizumoto K, Murakami M, Qian LW, Sato N, Nagai E, et al. Radiation to stromal fibroblasts increases invasiveness of pancreatic cancer cells through tumor-stromal interactions. Cancer Res. 2004; 64(9):3215–22. [PubMed: 15126362]

14. Placencio VR, Li X, Sherrill TP, Fritz G, Bhowmick NA. Bone marrow derived mesenchymal stem cells incorporate into the prostate during regrowth. PLoS One. 2010; 5(9):e12920. Epub 2010/10/05. [PubMed: 20886110]

15. Ahles TA, Saykin AJ. Candidate mechanisms for chemotherapy-induced cognitive changes. Nat Rev Cancer. 2007; 7(3):192–201. [PubMed: 17318212]

16. Massague J. TGFbeta signalling in context. Nat Rev Mol Cell Biol. 2012; 13(10):616–30. Epub 2012/09/21. [PubMed: 22992590]

17. Kim SJ, Im YH, Markowitz SD, Bang YJ. Molecular mechanisms of inactivation of TGF-beta receptors during carcinogenesis. Cytokine Growth Factor Rev. 2000; 11(1–2):159–68. [PubMed: 10708963]

18. Li X, Placencio V, Iturregui JM, Uwamariya C, Sharif-Afshar AR, Koyama T, et al. Prostate tumor progression is mediated by a paracrine TGF-beta/Wnt3a signaling axis. Oncogene. 2008; 27(56): 7118–30. Epub 2008/08/30. [PubMed: 18724388]

19. Jackson RS 2nd, Placzek W, Fernandez A, Ziaee S, Chu CY, Wei J, et al. Sabutoclax, a Mcl-1 antagonist, inhibits tumorigenesis in transgenic mouse and human xenograft models of prostate cancer. Neoplasia. 2012; 14(7):656–65. Epub 2012/08/21. [PubMed: 22904682]

20. Hodge DR, Cho E, Copeland TD, Guszczynski T, Yang E, Seth AK, et al. IL-6 enhances the nuclear translocation of DNA cytosine-5-methyltransferase 1 (DNMT1) via phosphorylation of the nuclear localization sequence by the AKT kinase. Cancer genomics & proteomics. 2007; 4(6): 387–98. Epub 2008/01/22. [PubMed: 18204201]

21. Lee SO, Lou W, Hou M, de Miguel F, Gerber L, Gao AC. Interleukin-6 promotes androgen-independent growth in LNCaP human prostate cancer cells. Clin Cancer Res. 2003; 9(1):370–6. Epub 2003/01/23. [PubMed: 12538490]
22. Du Z, Song J, Wang Y, Zhao Y, Guda K, Yang S, et al. DNMT1 stability is regulated by proteins coordinating deubiquitination and acetylation-driven ubiquitination. Science signaling. 2010; 3(146):ra80. Epub 2010/11/04. [PubMed: 21045206]
23. Dakhova O, Ozen M, Creighton CJ, Li R, Ayala G, Rowley D, et al. Global gene expression analysis of reactive stroma in prostate cancer. Clin Cancer Res. 2009; 15(12):3979–89. Epub 2009/06/11. [PubMed: 19509179]
24. Sun Y, Campisi J, Higano C, Beer TM, Porter P, Coleman I, et al. Treatment-induced damage to the tumor microenvironment promotes prostate cancer therapy resistance through WNT16B. Nat Med. 2012; 18(9):1359–68. Epub 2012/08/07. [PubMed: 22863786]
25. Cahill DP, Kinzler KW, Vogelstein B, Lengauer C. Genetic instability and darwinian selection in tumours. Trends Cell Biol. 1999; 9(12):M57–60. [PubMed: 10611684]
26. Fearon ER, Cho KR, Nigro JM, Kern SE, Simons JW, Ruppert JM, et al. Identification of a chromosome 18q gene that is altered in colorectal cancers. Science. 1990; 247(4938):49–56. [PubMed: 2294591]
27. Tuxhorn JA, Ayala GE, Rowley DR. Reactive stroma in prostate cancer progression. J Urol. 2001; 166(6):2472–83. [PubMed: 11696814]
28. Maruyama R, Choudhury S, Kowalczyk A, Bessarabova M, Beresford-Smith B, Conway T, et al. Epigenetic regulation of cell type-specific expression patterns in the human mammary epithelium. PLoS Genet. 2011; 7(4):e1001369. Epub 2011/05/03. [PubMed: 21533021]
29. Krtolica A, Parrinello S, Lockett S, Desprez PY, Campisi J. Senescent fibroblasts promote epithelial cell growth and tumorigenesis: a link between cancer and aging. Proc Natl Acad Sci U S A. 2001; 98(21):12072–7. [PubMed: 11593017]
30. Dumont N, Wilson MB, Crawford YG, Reynolds PA, Sigaroudinia M, Tlsty TD. Sustained induction of epithelial to mesenchymal transition activates DNA methylation of genes silenced in basal-like breast cancers. Proc Natl Acad Sci U S A. 2008; 105(39):14867–72. Epub 2008/09/23. [PubMed: 18806226]
31. Kantarjian H, Giles F, List A, Lyons R, Sekeres MA, Pierce S, et al. The incidence and impact of thrombocytopenia in myelodysplastic syndromes. Cancer. 2007; 109(9):1705–14. Epub 2007/03/17. [PubMed: 17366593]
32. Kantarjian H, Issa JP, Rosenfeld CS, Bennett JM, Albitar M, DiPersio J, et al. Decitabine improves patient outcomes in myelodysplastic syndromes: results of a phase III randomized study. Cancer. 2006; 106(8):1794–803. Epub 2006/03/15. [PubMed: 16532500]
33. Shen H, Laird PW. In epigenetic therapy, less is more. Cell Stem Cell. 2012; 10(4):353–4. Epub 2012/04/10. [PubMed: 22482500]
34. Trobridge P, Knoblaugh S, Washington MK, Munoz NM, Tsuchiya KD, Rojas A, et al. TGF-beta receptor inactivation and mutant Kras induce intestinal neoplasms in mice via a beta-catenin-independent pathway. Gastroenterology. 2009; 136(5):1680–8. e7. Epub 2009/02/12. [PubMed: 19208363]
35. Grady WM, Willis J, Guilford PJ, Dunbier AK, Toro TT, Lynch H, et al. Methylation of the CDH1 promoter as the second genetic hit in hereditary diffuse gastric cancer. Nat Genet. 2000; 26(1):16–7. Epub 2000/09/06. [PubMed: 10973239]
36. Martinez-Ferrer M, Afshar-Sherif AR, Uwamariya C, de Crombrugghe B, Davidson JM, Bhowmick NA. Dermal transforming growth factor-beta responsiveness mediates wound contraction and epithelial closure. Am J Pathol. 2010; 176(1):98–107. Epub 2009/12/05. [PubMed: 19959810]
37. Li X, Martinez-Ferrer M, Botta V, Uwamariya C, Banerjee J, Bhowmick NA. Epithelial Hic-5/ARA55 expression contributes to prostate tumorigenesis and castrate responsiveness. Oncogene. 2010 Epub 2010/09/08.
38. Kiskowski MA, Jackson RS 2nd, Banerjee J, Li X, Kang M, Iturregui JM, et al. Role for stromal heterogeneity in prostate tumorigenesis. Cancer Res. 2011; 71(10):3459–70. Epub 2011/03/30. [PubMed: 21444670]

39. Weber M, Davies JJ, Wittig D, Oakeley EJ, Haase M, Lam WL, et al. Chromosome-wide and promoter-specific analyses identify sites of differential DNA methylation in normal and transformed human cells. Nat Genet. 2005; 37(8):853–62. Epub 2005/07/12. [PubMed: 16007088]

40. Oliveros, JC. 2007. http://bioinfogp.cnb.csic.es/tools/venny/index.html

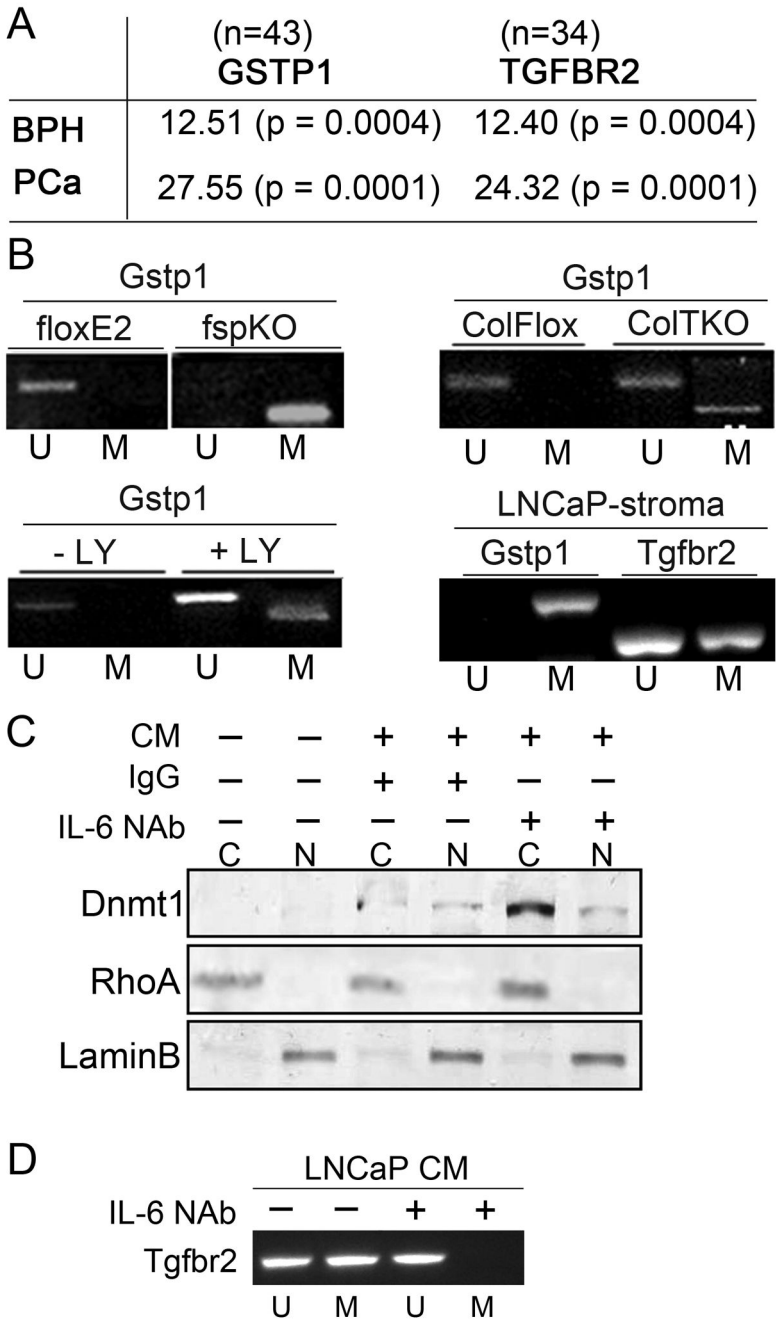

Figure 1. Prostate cancer mediate epigenetic changes in the associated stromal cells in a TGF-β-dependent manner

A. Promoter methylation analysis in BPH and PCa patient tissues support significant association between *GSTP1* and *TGFBR2* by Chi-square values and student T-test, in parenthesis. **B.** *Gstp1* promoter methylation status in the prostatic fibroblastic cells from $Tgfbr2^{floxE2/floxE2}$ and $Tgfbr2^{fspKO}$ mice were tested, as were $Tgfbr2^{ColTKO}$ prostatic stromal cells 72 hrs. following 4-OH tamoxifen-induced Cre activation by mPCR. Control $Tgfbr2^{floxE2/floxE2}$ fibroblasts treated with or without the TGF-β reptor type I inhibitor, LY364947 (24h), mediated *Gstp1* promoter methylation. Microdissected host CAF from

LNCaP xenografts were tested for mouse *Gstp1* and *Tgfbr2* promoter methylation. Unmethylated (U) and methylated (M) DNA is indicated. **C.** Conditioned media (CM) from LNCaP cells was incubated with $Tgfbr2^{floxE2/floxE2}$ fibroblasts for 2 days in the presence or absence of IgG and IL-6 neutralizing antibody (NAb). Cytoplasmic (C) and nuclear (N) fractions were Western blotted for Dnmt1 expression. RhoA and LaminB expression was used as loading controls for cytoplasmic and nuclear fractions, respectively. **D.** *Tgbr2* promoter methylation status of prostatic fibroblasts by mPCR following LNCaP conditioned media incubation in the presence or absence of IL-6 NAb. The mPCR data in this figure is representative of six independent experiments with a significant densitometric difference between the treatment and control groups ($p < 0.0001$).

A

	DNMT1 activity (U/μg protein)	DNMT3b activity (U/μg protein)
Pos. Control	240	238
Tgfbr2$^{floxE2/floxE2}$	34.69	50.44
Tgfbr2^{fspKO}	132.56	64.50
NAF	10.5	37.13
CAF	49.88	20.25

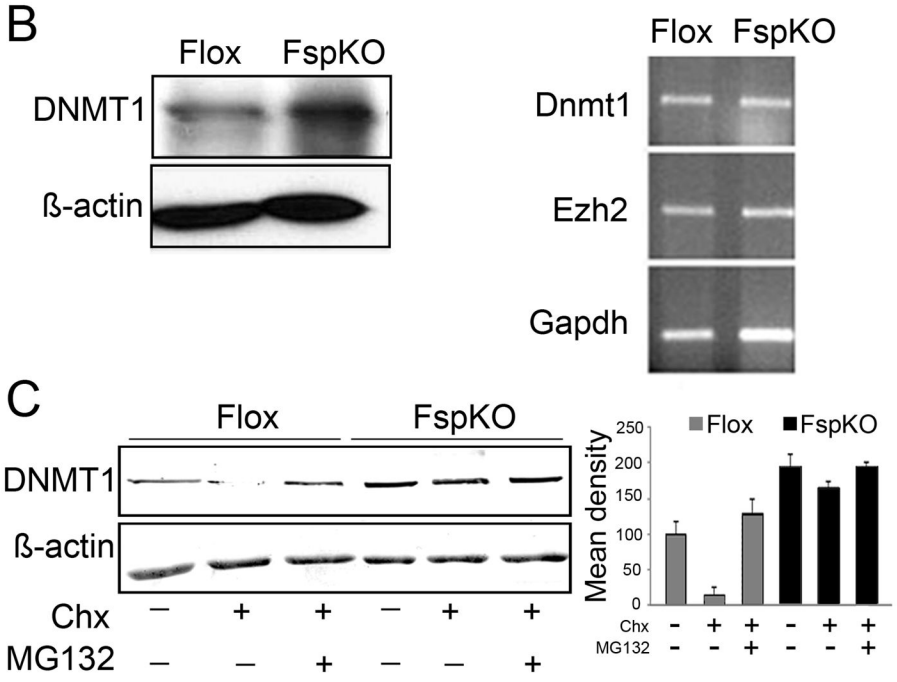

Figure 2. Post-translational regulation of DNMT1 expression

A. DNMT1 and DNMT3b activity was tested in Tgfbr2$^{floxE2/floxE2}$ and Tgfbr2^{fspKO} mouse prostatic stromal cells as well as human CAF and NAF cells. **B.** Western blotting indicated elevated DNMT1 protein expression in Tgfbr2^{fspKO}, compared to Tgfbr2$^{floxE2/floxE2}$ prostatic fibroblastic cells. However, RNA expression of DNMT1 and EZH2 were similarly expressed in Tgfbr2$^{floxE2/floxE2}$ and Tgfbr2^{fspKO} prostatic fibroblastic cells. **C.** Cyclohexamide (Chx) treatment resulted in the down regulation of DNMT1 protein expression in Tgfbr2$^{floxE2/floxE2}$ prostatic fibroblasts. Antagonizing proteosome activity (MG132) restored DNMT1 expression in Chx treated cells. DNMT1 protein expression was unaffected by Chx or MG-132 in Tgfbr2^{fspKO} prostatic fibroblasts. Columns in the graph are mean and SD of six densitometric readings adjusted for actin in independent blots prepared from three randomly-selected samples per treatment group ($p < 0.0001$).

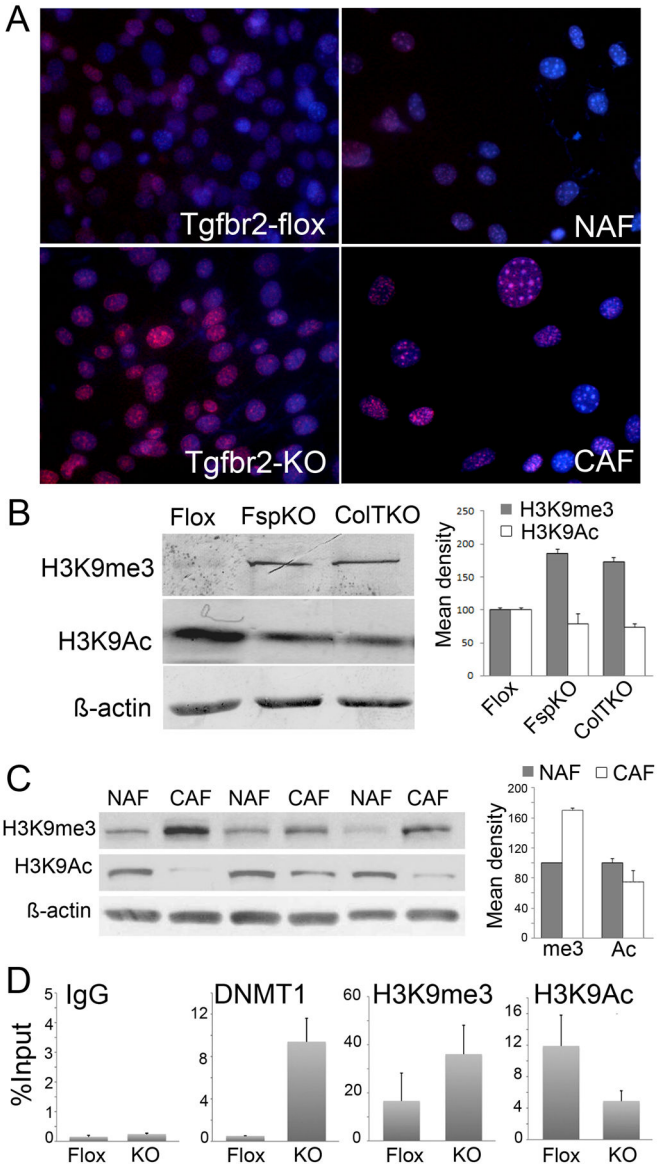

Figure 3. Stromal histone and chromatin modification

A. H3K9me3 was immuno-localized in cultured mouse Tgfbr2-flox and Tgfbr2-KO prostatic fibroblasts as well as human NAF and CAF (red). Nuclei were counter stained with Hoechst (blue). **B.** H3K9me3 and H3K9Ac3 expression in prostatic fibroblastic cells from $Tgfbr2^{floxE2/floxE2}$ and $Tgfbr2^{fspKO}$ mice, as well as those from $Tgfbr2^{ColTKO}$ mice 72 hours following tamoxifen-induced Cre activation were compared to β-actin loading control by Western blotting. Semi-quantitative densitometry of the bands from three independent Western blots showed significant differences in Tgfbr2-KO and Tgfbr2-Flox fibroblasts ($p<0.0001$). **C.** Protein expression of H3K9me3 and H2K9Ac in NAF and CAF differed significantly ($p<0.001$). Columns in the graph are mean values and standard deviation of six independent samples of NAF and CAF (only 3 of each are shown) adjusted for actin expression. **D.** DNMT1, H3K9me3, and H3K9Ac loading on the *Gstp1* promoter were

measured by ChIP analysis in Tgfbr2-flox and Tgfbr2-KO prostatic stromal cells by qPCR, relative to input DNA. Nonspecific IgG was used as a negative control.

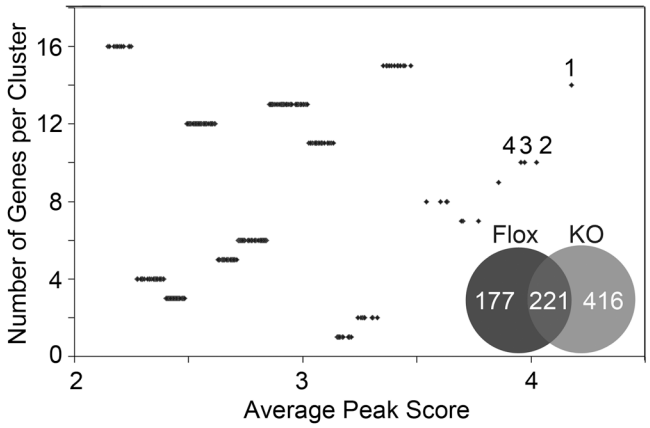

Cluster 1	Cluster 2	Cluster 3	Cluster 4
Spink2	Brca1	Hspa1a	Ercc6
Parp16	PolB	Hspa1b	Slc6a7
Fcgr3	Slc37a1	Spatc1	Mta2
Amn	Mizf	Zbtb38	Snag1
Smug1	Derl3	Sox6	Hist1h1t
Gstp1	Gpr178	Cmah	Lif
Neil 1	Rad50	Commd4	Klhl26
Neil 2	Rad54	Lsp1	Cdkn1c
Gm52	Podxl2	Rpa1	Sumo2
Pctk2	Hcst	Ercc4	Zfp513
Pdlim1			
Efcbp2			
Dmc1			
Gtf2h2			

Figure 4. Promoter methylation in prostatic fibroblast occur in a TGF-β-dependent manner

Methylation array revealed differences in Tgfbr2-KO (grey) and Tgfbr2-flox (black) prostatic fibroblasts. The Venn diagram illustrates the distribution of methylated genes in the two fibroblastic cell types validated by two independent array platforms. Cluster analysis indicated differential methylation of DNA-damage repair genes (underlined text, statistical significance set at p-value ≤ 0.05), with a summary of the specific gene names corresponding to the numbered clusters having the greatest peak scores.

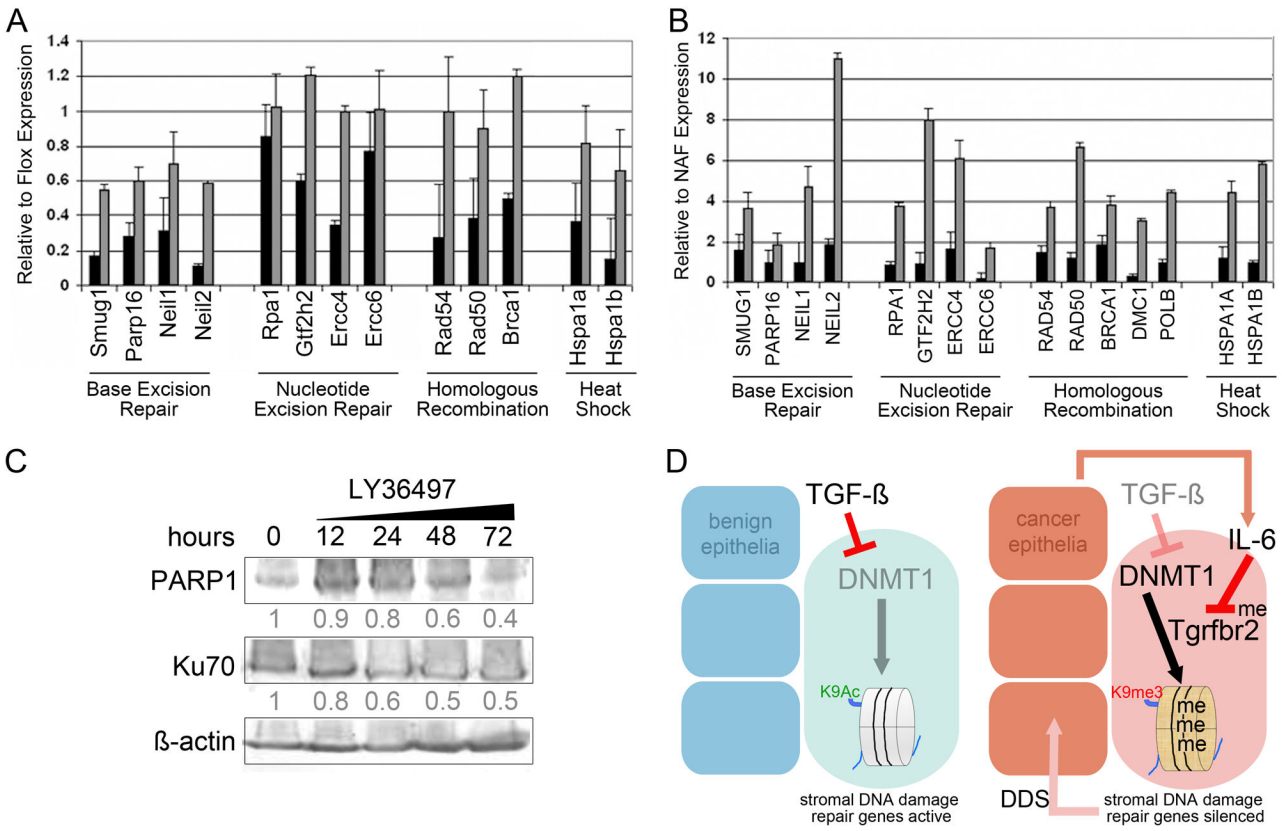

Figure 5. Prostatic mouse Tgfbr2-KO and human CAF silencing of DNA damage repair genes are reversible by 5-aza-dC treatment

RNA expression of DNA damage repair genes were measured by qPCR. **A.** The expression in Tgfbr2-KO as compared to Tgfbr2-flox mouse fibroblastic cells following vehicle (black bars) and 5-aza-dC treatment (grey bar) was used to determine if promoter methylation affected gene silencing. All genes shown were significantly regulated by DNA methylation ($p < 0.01$), except *Rpa1* and *Ercc6*. **B.** The expression of human homologs of the mouse genes were tested in CAF, as compared to NAF, following treatment with vehicle or 5-aza-dC. All genes shown were significantly regulated by DNA methylation ($p < 0.01$). **C.** Antagonizing TGF-β by LY36497 treatment of human NAF indicate regulation of PARP1 and Ku70 expression in a time course of 0 – 72 by Western blotting. The densitometry of the blots indicate relative PARP1 and Ku70 expression normalized to β-actin. **D.** A summary of our understanding of the mechanism by which stromal co-evolution contributes to a vicious cycle of stromal-epithelial interaction in cancer progression. The down regulated pathways are dimmed and active signaling are highlighted.

Table 1

Restoring DNA damage repair capacity of prostatic stromal cells limits tumor inductivity

A. C42b cells were orthotopically grafted alone or in tissue recombination with wild type mouse fibroblasts that were irradiated and/or treated with 5-aza-dC (see Supplemental Figure 3). **B.** LNCaP epithelia were grafted alone or in tissue recombination with untreated or 5-aza-dC treated Tgfbr2-KO prostatic fibroblastic cells (see Supplemental Figure 4). The mean tumor volume and mitotic index are indicated with 95% confidence interval and p value for each condition.

A

		epithelia only	epithelia + stroma	epithelia + 8Gy stroma	epithelia + 5-azDC, 8Gy stroma
Tumor Vol.	Mean	156.33	269.71	329.33	78.60
	CI 95%	31.93–58.74	38.65–56.20	28.43–38.69	28.48–39.69
	p value	<0.0001	0.2015	0.0415	0.0021
Proliferation	Mean	45.33	47.43	54.93	34.06
	CI 95%	101.88–210.77	234.08–305.35	299.94–367.83	31.35–125.85
	p value	<0.0001	<0.0001	0.0003	0.0085

B

		epithelia only	epithelia + Tgfbr2-KO stroma	epithelia + 5 aza DC Tgfbr2-KO stroma
Tumor Vol.	Mean	10.33	21.40	6.00
	CI 95%	8.82–11.85	20.23–22.57	4.83–7.17
	p value	<0.0001	<0.0013	<0.0001
Proliferation	Mean	11.00	21.0	5.8
	CI 95%	9.11–12.9	18.33–22.7	4.12–7.55
	p value	<0.0001	<0.0001	<0.0024